

Wednesday 25 Nov

Plasma FIB-SEM for multi-modal materials characterization

Free webinar

16.15-17.15 CET | 10.15-11.15 EST

[Register here](#)



Dean Miller
Senior Scientist,
Tescan

Wiley Analytical Science



Rechargeable Calcium–Sulfur Batteries Enabled by an Efficient Borate-Based Electrolyte

Zhenyou Li, Bhaghavathi Parambath Vinayan, Thomas Diemant, Rolf Jürgen Behm, Maximilian Fichtner, and Zhirong Zhao-Karger*

Rechargeable metal–sulfur batteries show great promise for energy storage applications because of their potentially high energy and low cost. The multivalent-metal based electrochemical system exhibits the particular advantage of the feasibility of dendrite-free metal anode. Calcium (Ca) represents a promising anode material owing to the low reductive potential, high capacity, and abundant natural resources. However, calcium–sulfur (Ca–S) battery technology is in an early R&D stage, facing the fundamental challenge to develop a suitable electrolyte enabling reversible electrochemical Ca deposition, and at the same time, sulfur redox reactions in the system. Herein, a study of a room-temperature Ca–S battery by employing a stable and efficient calcium tetrakis(hexafluoroisopropoxy) borate $\text{Ca}[\text{B}(\text{hfip})_4]_2$ electrolyte is presented. The Ca–S batteries exhibit a cell voltage of ≈ 2.1 V (close to its thermodynamic value) and good reversibility. The mechanistic studies hint at a redox chemistry of sulfur with polysulfide/sulfide species involved in the Ca-based system.

The use of clean renewable energy resources in stationary applications and emission-free transportation is imperative for the modern society due to the ever-growing demand for energy consumption accompanied by environmental pollution and climate change. Therefore, an implementation of efficient and cost-effective energy storage technology is necessary. Rechargeable batteries technology represents a feasible solution for a series of energy storage applications. Lithium-ion batteries (LIBs) are the main power sources for today's portable electronic devices and emerging electric vehicles.

Dr. Z. Li, Dr. B. P. Vinayan, Prof. M. Fichtner, Dr. Z. Zhao-Karger
Helmholtz Institute Ulm (HIU) Electrochemical Energy Storage
Helmholtzstraße 11, Ulm D-89081, Germany
E-mail: Zhirong.Zhao-Karger@kit.edu

Dr. T. Diemant, Prof. R. J. Behm
Institute of Surface Chemistry and Catalysis
Ulm University
Albert-Einstein-Allee 47, Ulm D-89081, Germany

Prof. M. Fichtner
Institute of Nanotechnology
Karlsruhe Institute of Technology (KIT)
Hermann-von-Helmholtz-Platz 1, Eggenstein-Leopoldshafen,
D-76344, Germany

 The ORCID identification number(s) for the author(s) of this article can be found under <https://doi.org/10.1002/smll.202001806>.

© 2020 The Authors. Published by Wiley-VCH GmbH. This is an open access article under the terms of the Creative Commons Attribution License, which permits use, distribution and reproduction in any medium, provided the original work is properly cited.

DOI: 10.1002/smll.202001806

However, to meet the requirements for global e-mobility and grid-scale electricity storage, new battery chemistries may help to relieve pressure from the critical raw material resources that are employed in the LIBs. Moreover, there is the chance to overcome intrinsic limitations in terms of energy density, cost, effectiveness and raw material sustainability of current systems.^[1–3] Multivalent metal-based batteries are receiving considerable attention as post-lithium technologies owing to their potential advantages with respect to high energy density, cost effectiveness and safety features.^[4–9]

Ca is the fifth most abundant element in the earth's crust and the resources are evenly distributed throughout the world. Ca has a high volumetric capacity of 2073 mAh cm⁻³ and a reduction potential of -2.87 V versus SHE, which is close to

that of Li (-3.04 V vs SHE) and 0.5 V lower than that of magnesium (Mg, -2.37 V vs SHE). Thus, the theoretical cell voltage and energy density of a Ca battery is comparable to Li-based systems, and yet higher than that of Mg batteries. In addition, doubly charged Ca²⁺ ion exhibits a relatively low charge density owing to its relatively large radius (1.12 Å), which may lead to faster Ca-ion diffusion kinetics than Mg²⁺-ion (with a radius 0.72 Å). However, the development of Ca batteries is hampered by the lack of a suitable electrolyte, which is capable of efficient ion transfer and does not form surface blocking layer on Ca metal.^[7,9,10] At the same time, there is high demand for viable cathode materials capable of reversible Ca-ion intercalation in order to create a feasible rechargeable Ca battery.^[7–9,11–14] As a low-cost, sustainable and environmentally benign material, sulfur (S) is a very appealing cathode material for next-generation batteries. Elemental sulfur can undergo two-electron redox reaction and offer a theoretical specific capacity of 1672 mAh g⁻¹, which is approximately ten times more than those of the common intercalation cathodes in LIBs. Due to the relatively low oxidation potential of sulfur, coupling with a metal anode is necessary for achieving a high energy density of a sulfur-based battery. Metal-sulfur batteries offer considerable potential for low-cost and high-energy storage.^[15] Lithium–sulfur (Li–S) battery has been extensively investigated in the past decade.^[16] However, one of the biggest technical challenges is to cope with the dendrite growth on the Li-metal anode, which can cause internal short circuit and explosion hazards during cycling the batteries.^[17] Similarly, the commercialization of room-temperature sodium–sulfur (Na–S) batteries also needs

to address the intrinsic problems associated with high reactivity and severe dendrite growth on the use of metallic Na anode.^[18] On the contrary, the inherent characteristics of alkaline earth metals, e.g., magnesium (Mg) and calcium (Ca) as a safe metal anode render the Mg–S and Ca–S batteries particularly advantageous.^[10,19–27] To achieve an energy dense system, Ca would be an ideal anode to couple with sulfur. Based on a two-electron conversion reaction described as $\text{Ca}^{2+} + \text{S} + 2\text{e}^- \leftrightarrow \text{CaS}$, on the basis of the Gibbs energy ($\Delta_r G$) of $-4774 \text{ kJ mol}^{-1}$ for the formation of CaS, the redox couple exhibits a theoretical cell voltage of 2.47 V with respect to $\text{Ca}^{2+}/\text{Ca}^0$. The Ca–S battery could theoretically provide a volumetric energy density of 3202 Wh L^{-1} (1835 Wh kg^{-1} on a weight basis), which is comparable to that of a Mg–S system, yet beyond that of a Li/S battery (2800 Wh L^{-1}).

The prerequisite for the development of metal-sulfur batteries is to discover a proper electrolyte, which exhibits sufficient oxidative stability and chemical compatibility with both of the metal anode and sulfur cathode. In the past several years, substantive progress has been made in the investigation of Mg–S batteries by employing stable and effective Mg electrolytes,^[19,21,28–30] whereas absence of a suitable electrolyte is still a bottleneck for the research on Ca–S batteries.^[7,9,10] A primary calcium–sulfur cell has been tested using an electrolyte solution of calcium perchlorate [$\text{Ca}(\text{ClO}_4)_2$] in acetonitrile (CH_3CN), with a high discharge capacity of 600 mAh g^{-1} .^[10] Recently, another attempt at the rechargeable Ca–S battery indicated that an electrolyte solution of calcium trifluoromethanesulfonate [$\text{Ca}(\text{CF}_3\text{SO}_3)_2$] in glyme is also incapable of enabling the reversible electrochemical reaction in the system.^[26] In both cases, the inability of the employed electrolytes was supposed to be responsible for the irreversibility of the Ca–S batteries. It was further reported that the recharge process in the Ca–S cells may be facilitated through a so-called Li-ion mediator approach by incorporating 0.5 M of lithium trifluoromethanesulfonate (LiCF_3SO_3) with 0.2 M of $\text{Ca}(\text{CF}_3\text{SO}_3)_2$ solution in tetraglyme.^[26] The cells could be cycled for 20 times delivering reversible discharge capacity of $\approx 300 \text{ mAh g}^{-1}$ at a current rate of C/10. However, these cells displayed a low average discharge voltage of ($<1 \text{ V vs Ca}^{2+}/\text{Ca}$), which is far below the thermodynamic electromotive force (emf) of 2.43 V, thus reducing the potentially high energy of the Ca–S battery to less than half its theoretical value. In addition, the formation of lithium sulfide (Li_2S) in this electrochemical system implies a consumption of LiCF_3SO_3 in the electrolyte during discharge. Such cells would require large amount of electrolyte and the consumption of the mediator leads to the loss of capacity and limited lifetime of the batteries.

Numerous studies of metal-sulfur batteries have suggested that the electrolyte is the main factor determining the electrochemical performance of the cells.^[31] It is therefore of paramount importance to develop a more suitable electrolyte that is capable of enabling an effective ion transfer and does not form passivation layers on Ca anode. Recently, a new class of Ca salts with weakly coordinating anions has been introduced as a first efficient room-temperature electrolyte for non-aqueous Ca batteries.^[32,33] These $\text{Ca}[\text{B}(\text{hfp})_4]_2$ based electrolytes exhibit electrochemical properties of a state-of-the-art electrolyte system in terms of easy synthesis, high oxidative stability of 4.5 V, high ionic conductivity of $\approx 8 \text{ mS cm}^{-1}$ and efficient reversible Ca deposition.^[32] The outstanding electrochemical properties and its chemical compatibility make the

electrolyte well-suited for the investigation of sulfur and other high-voltage cathodes for Ca batteries. In this study, we for the first time present the electrochemical performance of Ca–S batteries with $\text{Ca}[\text{B}(\text{hfp})_4]_2$ electrolyte, demonstrating reversible Ca–S cells with a discharge voltage close to its thermodynamic value. Moreover, the analysis of the reversible S^0/CaS redox chemistry reveals that the dissolution of the polysulfides and passivation of the Ca anode are major causes for the capacity fade.

The sulfur/carbon (S/C) composite cathode was prepared by incorporating elemental sulfur in a conductive carbon material (Ketjenblack, KB) by a melt-diffusion method (see the Supporting Information). Morphological and crystallographic measurements showed that the sulfur was uniformly distributed on the carbon support (Figure S2, Supporting Information). $\text{Ca}[\text{B}(\text{hfp})_4]_2$ was readily synthesized through the one-step reaction of $\text{Ca}(\text{BH}_4)_2$ and hexafluoroisopropanol (hfp-H) according to our previous report.^[32] The Ca borate electrolyte solution was made by simply dissolving $\text{Ca}[\text{B}(\text{hfp})_4]_2$ salt in proper amount of dimethoxyethane (DME). The Ca–S batteries were tested by coupling the S/C cathode with a pressed Ca pellet as anode in 0.25 M $\text{Ca}[\text{B}(\text{hfp})_4]_2/\text{DME}$ electrolyte.

Figure 1a shows discharge/charge curves with three stages: a flat plateau at 2.1 V, a slope at around 1.5 V and another slope in the low voltage range at 1 V, indicating a multistep reaction. A discharge capacity of about 760 mAh g^{-1} was delivered in the voltage window between the open circuit voltage (OCV) of 2.5 V and the cut-off at 1 V while the charge capacity far exceeds the discharge capacity, implying a polysulfide shuttling effect, as is known from other metal-sulfur systems.^[34] In fact, the formation of polysulfides was confirmed by ultraviolet–visible (UV/Vis) spectroscopic analysis of the electrolyte after the first discharge. The electrolyte was extracted by immersing the separator in a proper amount of DME. Compared to the neat electrolyte, the main absorbance peak emerged at about 230 nm with a shoulder peak at 270 nm (Figure S3, Supporting Information), which could be assigned to high-order polysulfide species (S_8^{2-} , S_6^{2-}). Another broad peak at 303 nm might be attributed to low-order polysulfide species such as S_4^{2-} .^[19,35] Note that the intensities of peaks correspond to S_6^{2-} and S_4^{2-} are even higher in the charge state than those in the discharge state, indicating a continuous leaching of the sulfur species. The dissolution of polysulfides lead to a loss of active material, which affects the cycling stability of the Ca/S cells so that a capacity of about 120 mAh g^{-1} remained after 15 cycles (Figure 1b).

Cyclic voltammograms (CVs) were measured using S/C working electrodes (WE) and the Ca pellets as both counter and reference electrode (CE and RE). The CV profiles shown in Figure 1c display two main reduction peaks, which are present at around 2.28, 2.03 V and a broad signal at about 1.08 V during the first cathodic scan. This is almost consistent with the discharge profiles of the cells. According to the reported mechanistic studies on other metal-sulfur chemistries,^[19,21,30] the cathodic peaks at high voltage $>2 \text{ V}$ can be correlated to the reduction of elemental sulfur to high-order Ca polysulfides (CaS_x , $4 \leq x \leq 8$) and the peaks at lower voltages might correspond to the reduction of high-order CaS_x to low-order Ca polysulfides with the formation of CaS_2 and CaS. Owing to the fast kinetics of the reduction of elemental sulfur to higher order polysulfides, we attribute their stepwise reactions in the high voltage range to the plateau at 2.1 V

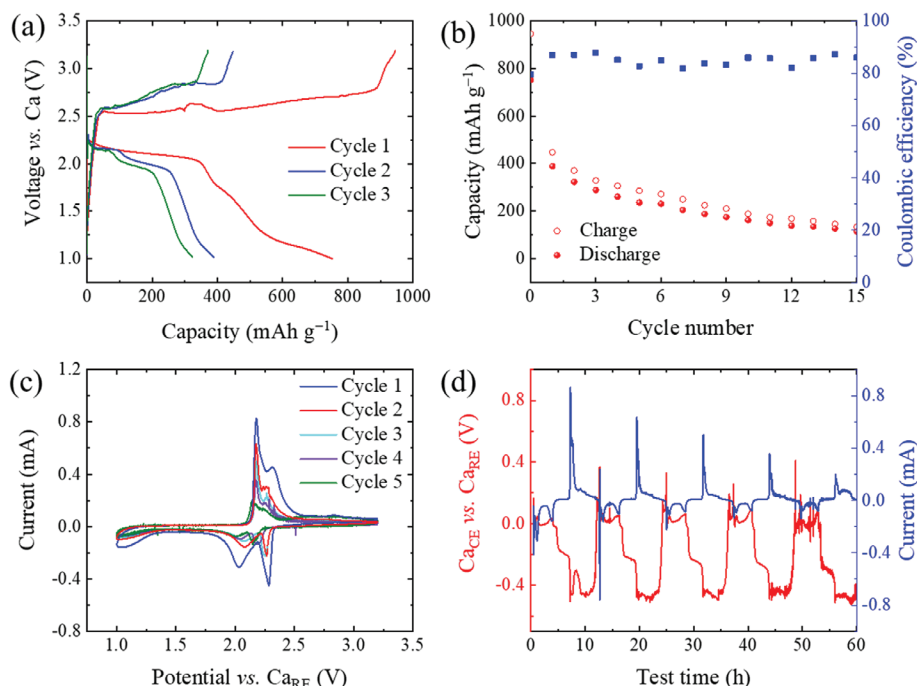


Figure 1. Electrochemical performance of the Ca–S batteries with the $\text{Ca}[\text{B}(\text{hfp})_4]_2/\text{DME}$ electrolyte in a voltage window of 1.0–3.2 V: a) charge-discharge profiles; b) cycling performance; c) CVs of the S/C WE using Ca as both CE and RE at a scan rate of 0.1 mV s^{-1} ; d) potential evolution of the Ca_{CE} versus Ca_{RE} and the current wave of the S/C WE versus scan time.

in the discharge profile. In the successive anodic scan, the two main oxidation peaks present at about 2.18 and 2.30 V (vs Ca_{RE}), which may be associated with the transformation of CaS and CaS_2 to the polysulfides CaS_x ($x > 2$) and finally the elemental sulfur, respectively. The CV curves from the second cycle up show that the redox pairs are still present; however, the intensities of current responses are substantially lower than that of the initial scan, reflecting the loss of sulfur in the WE. Besides, the spikes in the CV curves could be ascribed to the passivation of the Ca_{CE} by the dissolved polysulfides. Additionally, the potential evolution of Ca_{CE} versus Ca_{RE} as shown in Figure 1d indicates that a large polarization of $\approx 0.5 \text{ V}$ during the cathodic process, which suggests that the high activation energy barrier for recharging the Ca–S cells is most likely due to the passivation of the Ca counter electrode.

It should be highlighted that the high voltage ($> 2 \text{ V}$) presented here by applying $\text{Ca}[\text{B}(\text{hfp})_4]_2/\text{DME}$ electrolyte is two times higher than those reported in the literature^[10,26] under similar working conditions. The high voltage value, which is close to the theoretical emf value, demonstrates the feasibility of the new electrolyte for the Ca–S systems. However, similar as reported in other Ca–S systems,^[10,26] severe capacity fading upon repeated cycling has been observed, which is most likely caused by the dissolution of the polysulfide species and degradation of the Ca anode.

In fact, the post-mortem analysis of the cells after cycling by means of scanning electron microscopy (SEM) and energy-dispersive X-ray spectroscopy (EDX) revealed extensive morphological and chemical changes of the Ca surface after the first cycle. As shown in Figure 2a,b, freshly polished Ca anode has smooth surface with low oxygen content. In the fully discharged

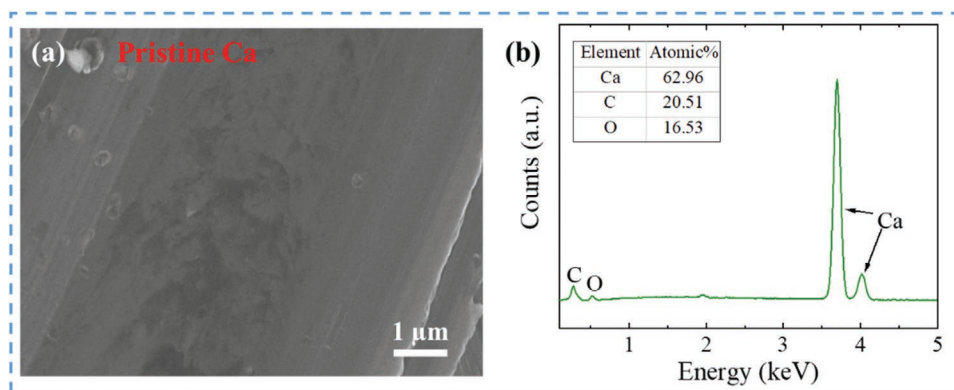


Figure 2. Characterization of the Ca anode before and after cycling. Pristine Ca anode: a) SEM image and b) EDX spectrum.

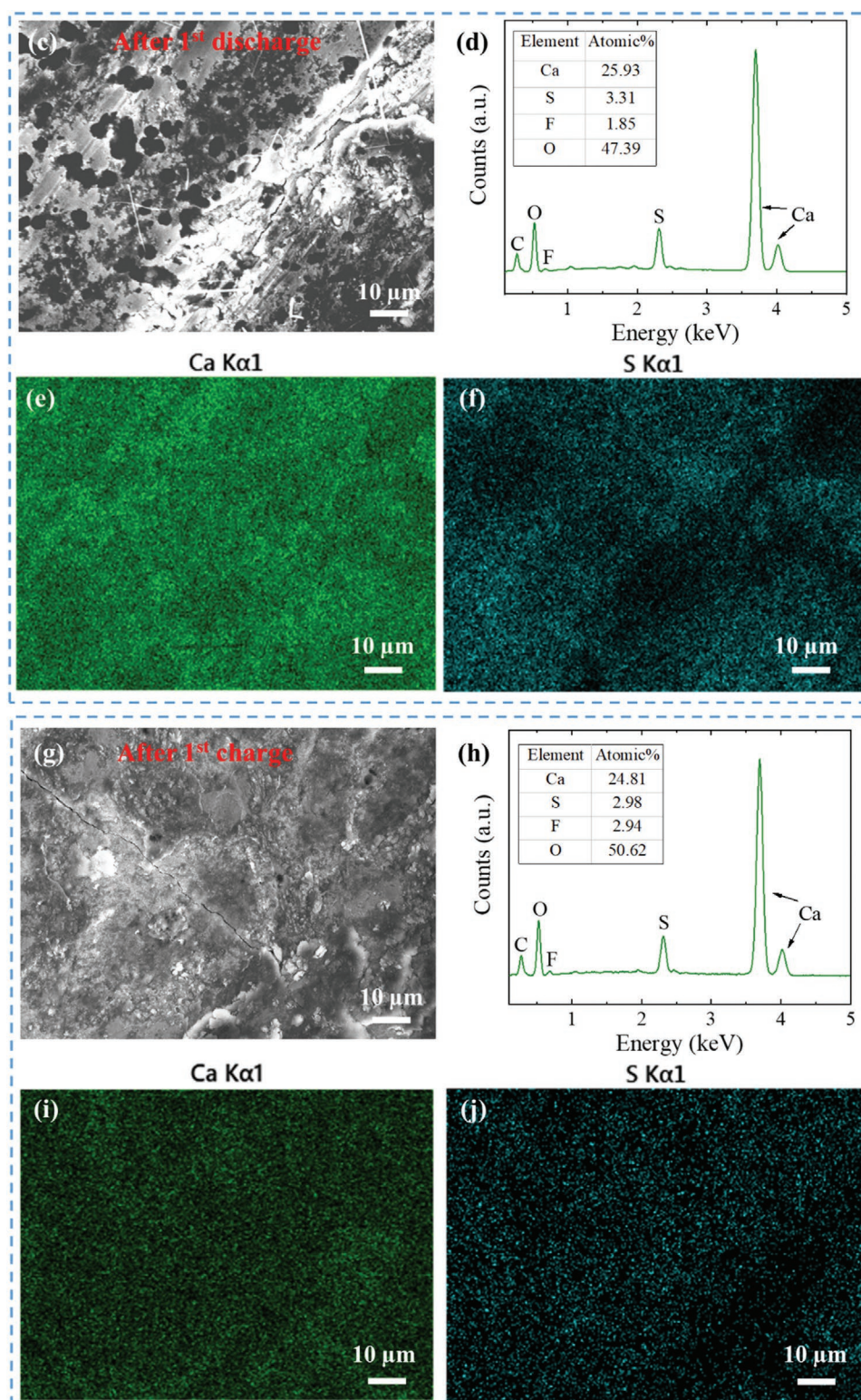


Figure 2. Continued. Ca anode after 1st discharge: c) SEM image, d) EDX spectrum, and e,f) corresponding Ca and S mapping. Ca anode after 1st charge: g) SEM image, h) EDX spectrum, and i,j) corresponding Ca and S mapping.

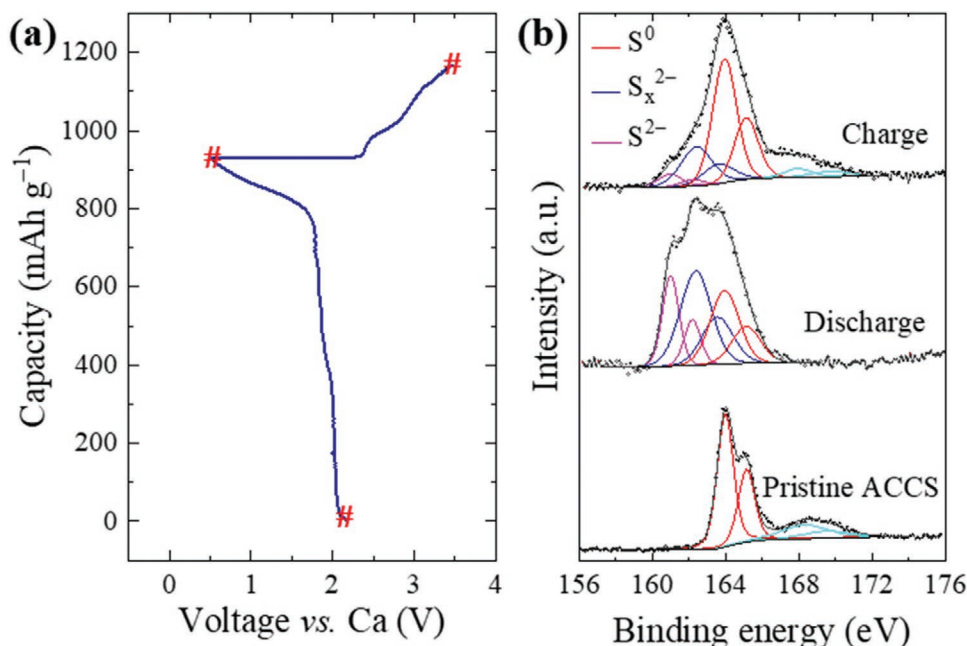


Figure 3. a) Voltage profiles of cycling ACCS cathode with the Ca[B(hfip)₄]₂/DME electrolyte in a voltage window of 0.5–3.4 V at a current rate C/20; b) XPS S 2p spectra of the sulfur cathodes at different electrochemical states.

state (Figure 2c), evenly distributed caves appear on the Ca surface, indicating a relatively homogeneous stripping of Ca. The corresponding EDX spectrum as well as elemental mapping in Figure 2d–f reveal sulfur species emerging at the Ca surface. The emergence of the sulfur species on the Ca anode even after the first discharge clearly implies the chemical passivation of Ca by the dissolved polysulfide. As Ca is a highly reactive alkaline earth metal and the polysulfide is thermodynamically unstable, the Ca metal anode is prone to spontaneously forming a surface layer via a side reaction with the polysulfide. The surface layer is hardly removed during the subsequent charging process as evidenced in Figure 2g–j. From the EDX spectrum, S/Ca ratio does not decrease dramatically compared to the fully discharged state, implying an immobilization of S at the anode side. The passivation of Ca anode may account for the large over potential in the discharge and charge processes and could also be a major reason for the limited cycling stability of Ca–S cells.

To gain insight into the reaction mechanism of the Ca–S battery chemistry, we examined the change of the oxidation state of sulfur upon discharge and charge by X-ray photoelectron spectroscopy (XPS). For these measurements, we prepared a binder-free activated carbon cloth/sulfur cathode (ACCS), which was discharged and charged at C/20 in a voltage window between 0.5 and 3.4 V. Figure 3a shows the voltage profile of the ACCS in the first cycle. It is worth to mention that ACCS showed an inferior cycle life compared to that of the S/C cathodes (Figure S4 in the Supporting Information). A possible reason for the inferior lifetime could be due to large active material-electrolyte interfaces by using the ACC/S cathode, which lead to faster dissolution of S and therefore quicker passivation of the Ca anode. Nevertheless, it was conveniently used for XPS because it would not have any influence of a binder. The S 2p spectra were fitted using spin-orbit splitting doublets with a binding energy

separation of 1.2 eV and an intensity ratio 2: 1, representing the 2p_{3/2} and 2p_{1/2} components of the doublet, respectively (Figure 3b). The spectra of the pristine ACCS cathode display the characteristic doublet of elemental sulfur at 164.1/165.3 eV. The smaller and relatively broad feature at higher binding energy (≈168–169 eV) can be attributed to oxidized S species and was also observed in other studies.^[30] After discharge to 0.5 V, the S 2p signal could be deconvoluted into three doublet peaks. The substantial decrease in intensity of the signals for elemental sulfur indicates the reduction of the sulfur cathode; whereas the signals at 161.0/162.2 eV can be assigned to CaS and the doublet at 162.4/163.6 eV to the terminal S atoms of the disulfide CaS₂ and polysulfides CaS_x (2 < x < 8), reflecting the effective conversion of sulfur to sulfides. Upon recharging to 3.4 V, the peaks for S₈ were restored to a large extent while the signals for the sulfides (CaS/CaS_x) diminished. The XPS results prove the reversible conversion reaction between S⁰ and CaS in the Ca–S system with Ca[B(hfip)₄]₂ electrolyte, which involves multistep redox transformation processes of the polysulfide intermediates, similar to those in other metal-sulfur systems.^[19,21,36]

In summary, we present the feasibility study of the borate Ca[B(hfip)₄]₂ electrolyte for rechargeable Ca–S battery. It has been demonstrated for the first time that the Ca–S battery can deliver a discharge potential close to the thermodynamic value, and that cells can deliver a high initial capacity. The mechanistic study verifies the chemical reversibility of the S⁰/CaS_x (x = 2–8) redox chemistry in the Ca–S batteries with the borate electrolyte. The dissolution of polysulfide was identified. It leads to loss of active material and causes severe passivation of the Ca anode, thereby accounting for the capacity fading and the limited cycle life of the batteries. Further strategy of sulfur cathode design and especially surface protection of Ca anode is necessary for performance improvement of Ca–S

batteries. Most important, this study has confirmed the suitability of the $\text{Ca}[\text{B}(\text{hfp})_4]_2$ electrolyte for the application in Ca–S batteries. Owing to the outstanding electrochemical properties, easy synthesis and feasibility for further modification with solvent blend or additives, this type of electrolytes opens the pathway for making developments towards practical Ca–S battery technology.

Supporting Information

Supporting Information is available from the Wiley Online Library or from the author.

Acknowledgements

Reference [32] was corrected on September 25, 2020, after initial publication online. This project has received funding from the European Union's Horizon 2020 research and innovation programme via "E-MAGIC" project under grant agreement No 824066. This study is also supported by Bundesministerium für Bildung und Forschung (BMBF) of Germany via "MagSiMal" project (03XP0208). This work contributes to the research performed at CELEST (Center for Electrochemical Energy Storage Ulm-Karlsruhe) and was partly funded by the German Research Foundation (DFG) under Project ID 390874152 (POLiS – Post Lithium Storage Cluster of Excellence). Open access funding enabled and organized by Projekt DEAL.

Conflict of Interest

The authors declare no conflict of interest.

Keywords

calcium anodes, fluorinated borate electrolytes, rechargeable calcium–sulfur batteries

Received: March 18, 2020

Revised: June 24, 2020

Published online: August 18, 2020

-
- [1] A. Manthiram, *J. Phys. Chem. Lett.* **2011**, *2*, 176.
[2] D. Larcher, J. M. Tarascon, *Nat. Chem.* **2015**, *7*, 19.
[3] C. Vaalma, D. Buchholz, M. Weil, S. Passerini, *Nat. Rev. Mater.* **2018**, *3*, 18013.
[4] J. Muldoon, C. B. Bucur, T. Gregory, *Chem. Rev.* **2014**, *114*, 11683.
[5] A. Ponrouch, J. Bitenc, R. Dominko, N. Lindahl, P. Johansson, M. R. Palacin, *Energy Storage Mater.* **2019**, *20*, 253.
[6] A. El Kharbachi, O. Zavorotynska, M. Latroche, F. Cuevas, V. Yartys, M. Fichtner, *J. Alloys Compd.* **2020**, *817*, 153261.

- [7] M. E. Arroyo-de Dompablo, A. Ponrouch, P. Johansson, M. R. Palacin, *Chem. Rev.* **2019**, <https://doi.org/10.1021/acs.chemrev.9b00339>.
[8] D. Monti, A. Ponrouch, R. B. Araujo, F. Barde, P. Johansson, M. R. Palacin, *Front. Chem.* **2019**, *7*, 79.
[9] A. Ponrouch, M. R. Palacin, *Curr. Opin. Electrochem.* **2018**, *9*, 1.
[10] K. A. See, J. A. Gerbec, Y.-S. Jun, F. Wudl, G. D. Stucky, R. Seshadri, *Adv. Energy Mater.* **2013**, *3*, 1056.
[11] M. Wang, C. Jiang, S. Zhang, X. Song, Y. Tang, H.-M. Cheng, *Nat. Chem.* **2018**, *10*, 667.
[12] S. Wu, F. Zhang, Y. Tang, *Adv. Sci.* **2018**, *5*, 1701082.
[13] N. Wu, W. Yao, X. Song, G. Zhang, B. Chen, J. Yang, Y. Tang, *Adv. Energy Mater.* **2019**, *9*, 1803865.
[14] J. Lang, C. Jiang, Y. Fang, L. Shi, S. Miao, Y. Tang, *Adv. Energy Mater.* **2019**, *9*, 1901099.
[15] S.-H. Chung, A. Manthiram, *Adv. Mater.* **2019**, *31*, 1901125.
[16] A. Manthiram, Y. Fu, S.-H. Chung, C. Zu, Y.-S. Su, *Chem. Rev.* **2014**, *114*, 11751.
[17] D. Lin, Y. Liu, Y. Cui, *Nat. Nanotechnol.* **2017**, *12*, 194.
[18] D. Kumar, S. K. Rajouria, S. B. Kuhar, D. K. Kanchan, *Solid State Ionics* **2017**, *312*, 8.
[19] Z. Zhao-Karger, X. Zhao, D. Wang, T. Diemant, R. J. Behm, M. Fichtner, *Adv. Energy Mater.* **2015**, *5*, 1401155.
[20] Z. Zhao-Karger, M. Fichtner, *MRS Commun.* **2017**, *7*, 770.
[21] Z. Zhao-Karger, R. Liu, W. Dai, Z. Li, T. Diemant, B. P. Vinayan, C. Bonatto Minella, X. Yu, A. Manthiram, R. J. Behm, M. Ruben, M. Fichtner, *ACS Energy Lett.* **2018**, *3*, 2005.
[22] X. Hong, J. Mei, L. Wen, Y. Tong, A. J. Vasileff, L. Wang, J. Liang, Z. Sun, S. X. Dou, *Adv. Mater.* **2019**, *31*, 1802822.
[23] P. Wang, M. R. Buchmeiser, *Adv. Funct. Mater.* **2019**, *29*, 1905248.
[24] B. P. Vinayan, Z. Zhao-Karger, T. Diemant, V. S. K. Chakravadhanula, N. I. Schwarzburger, M. A. Cambaz, R. J. Behm, C. Kübel, M. Fichtner, *Nanoscale* **2016**, *8*, 3296.
[25] L. Kong, C. Yan, J.-Q. Huang, M.-Q. Zhao, M.-M. Titirici, R. Xiang, Q. Zhang, *Energy Environ. Mater.* **2018**, *1*, 100.
[26] X. Yu, M. J. Boyer, G. S. Hwang, A. Manthiram, *Adv. Energy Mater.* **2019**, *9*, 1803794.
[27] B. P. Vinayan, H. Euchner, Z. Zhao-Karger, M. A. Cambaz, Z. Li, T. Diemant, R. J. Behm, A. Gross, M. Fichtner, *J. Mater. Chem. A* **2019**, *7*, 25490.
[28] Z. Zhao-Karger, X. Zhao, O. Fuhr, M. Fichtner, *RSC Adv.* **2013**, *3*, 16330.
[29] Z. Zhao-Karger, M. E. Gil Bardaji, O. Fuhr, M. Fichtner, *J. Mater. Chem. A* **2017**, *5*, 10815.
[30] T. Gao, S. Hou, F. Wang, Z. Ma, X. Li, K. Xu, C. Wang, *Angew. Chem., Int. Ed.* **2017**, *56*, 13526.
[31] Y. Pan, S. Li, M. Yin, J. Li, *Energy Technol.* **2019**, *7*, 1900164.
[32] Z. Li, O. Fuhr, M. Fichtner, Z. Zhao-Karger, *Energy Environ. Sci.* **2019**, *12*, 3496.
[33] A. Shyamsunder, L. E. Blanc, A. Assoud, L. F. Nazar, *ACS Energy Lett.* **2019**, *4*, 2271.
[34] Y. V. Mikhaylik, J. R. Akridge, *J. Electrochem. Soc.* **2004**, *151*, A1969.
[35] G. Bieker, D. Diddens, M. Kolek, O. Borodin, M. Winter, P. Bieker, K. Jalkanen, *J. Phys. Chem. C* **2018**, *122*, 21770.
[36] A. Robba, A. Vizintin, J. Bitenc, G. Mali, I. Arčon, M. Kavčič, M. Žitnik, K. Bučar, G. Aquilanti, C. Martineau-Corcoss, A. Randon-Vitanova, R. Dominko, *Chem. Mater.* **2017**, *29*, 9555.